JKAU: Eng. Sci., **vol. 9**, pp. 59-75 (1417 A.H./1997 A.D.)

Comparative Studies of Hot-Wire Techniques for Moderate Intensity Flows

M.H. AL-BEIRUTTY, A.M. RADHWAN and A.M. KHALIFA
Mechanical Engineering Department, Faculty of Engineering, King Abdulaziz University, Jeddah, Saudi Arabia

ABSTRACT. Methods employing hot wire anemometer techniques in obtaining quantitative turbulence information in turbulent flows are numerous. These techniques, however, were tested in different flow geometries under different operating conditions. It is difficult to decide on a technique preference unless the different techniques are tested under similar operating conditions and flow geometry. It is the main objective of this study to compare the single-wire, x-wire, and triple-wire measurement techniques under the same operating conditions.

Measurements of mean velocity and Reynolds stress components were conducted at seven different axial locations downstream of the jet exit plane using the single-wire, x-wire, and triple-wire techniques. A computer controlled three-dimensional traverse mechanism in conjunction with a data acquisition software developed for turbulent flow measurements and analysis were utilized.

The results showed that the three hot wire techniques gave similar results for the mean velocity components $\bar{U}$, $\bar{V}$, $\bar{W}$ and the Reynolds stress components $\overline{u\,v}$, $\overline{u\,w}$, $\overline{v\,w}$ and u^2. This agreement, however, was not apparent when comparing the normal stresses v^2 and w^2, especially for the single-wire technique. A very close agreement was achieved when the normalized mean axial velocity, $\bar{U}/\bar{U}_c$ and the normalized turbulence intensity $u'/\bar{U}_c$ were compared with the data published in the literature. This resulted in a good confidence of the accuracy of the measurement techniques used.

1. Introduction

Most flows that are of practical interest are turbulent, complex, and three dimensional of moderate intensity levels such as those which occur in gas turbine applica-

tions. Basic studies of turbulent axisymmetric jets, jet impingement and jet interaction have received special attention from researchers in the field since they represent prototype flows for studying fundamental aspects and characteristics of turbulent flows.

Though the hot wire anemometer (HWA) and the laser doppler velocimeter represent the most commonly used techniques in the measurement of mean velocity and Reynolds stress components in turbulent flows, some researchers in the field prefer that measurements be made by means of HWA technique[1-3], when applicable, in low-to-moderate intensity flows. Methods employing hot wire anemometer techniques for measurements in turbulent flows are numerous. Some of these techniques rely on single wire rotation[4-7], on x-wire rotation[8,9], or on the use of a stationary triple-wire probe[10,11]. The single and x-wire probes provide simple measurement techniques in complex skewed turbulent flows, however, with one or two wires, one does not have enough information to solve for the instantaneous velocities, and hence time averaging is required. As the number of terms retained in the time average turbulence equation increases, the number of independent realizations required increases, thus the number of equations increases. Consequently, convergence of solution is not attainable. With a triple wire probe, however, one can deal with the instantaneous velocity components. Although the triple wire technique provides a more accurate approach for calculating mean and turbulence quantities, the measurement technique is tedious due to the large size of the probe, and the difficulty associated with the calibration procedure. These techniques have been tested in different flow geometries under different operating conditions. However, it is difficult to decide on a technique unless the different techniques are tested under the same operating conditions and same flow geometry.

In the present study, a comparison among the different HWA techniques is achieved by conducting measurements at different locations downstream of a free axisymmetric jet issuing from an orifice. A computer controlled three-dimensional traverse mechanism in conjunction with a data acquisition software developed by DANTEC for turbulent flow measurements were utilized. A computer code was developed by the authors to reduce and analyze the raw data for the three techniques according to the methods developed in the next section.

2. Theoretical Analysis

The hot-wire response equations utilized for the single-wire, x-wire, and triple-wire techniques are given below. The development of the mean and turbulence response equations for the three techniques are based on the empirical cooling law relationship for a linearized response.

$$E = S\ U_e \tag{1}$$

where E is the constant-temperature anemometer output linearized voltage response to an effective cooling velocity U_e, and S represents the slope of the wire calibration curve.

2.1 Single-Wire Technique

Al-Beirutty[12] has developed a new data reduction method based on the use of stationary normal wire and a single rotatable slant wire. The method is of general applicability to turbulent three dimensional flows with moderately high turbulence intensity. The expression for the effective cooling velocity is given in terms of the velocity components in wire-coordinates system as

$$U_e^2 = U_N^2 + k^2 U_p^2 + h^2 U_{BN}^2 \tag{2}$$

where k and h are the yaw and pitch sensitivity factors, respectively. The normal (U_N), parallel (U_P) and binormal (U_{BN}), velocity components in wire coordinates may be expressed in terms of velocity components across the wire and rotation angle λ as shown in Fig. 1, by

$$U_N = (U + u)\cos\alpha + [(V + v)\cos\lambda + (W + w)\sin\lambda]\sin\alpha \tag{2a}$$

$$U_P = -(U + u)\sin\alpha + [V + v)\cos\lambda + (W + w)\sin\lambda]\cos\alpha \tag{2b}$$

$$U_{BN} = -(V + v)\sin\lambda + (W + w)\cos\lambda \tag{2c}$$

where α is the wire inclination angle.

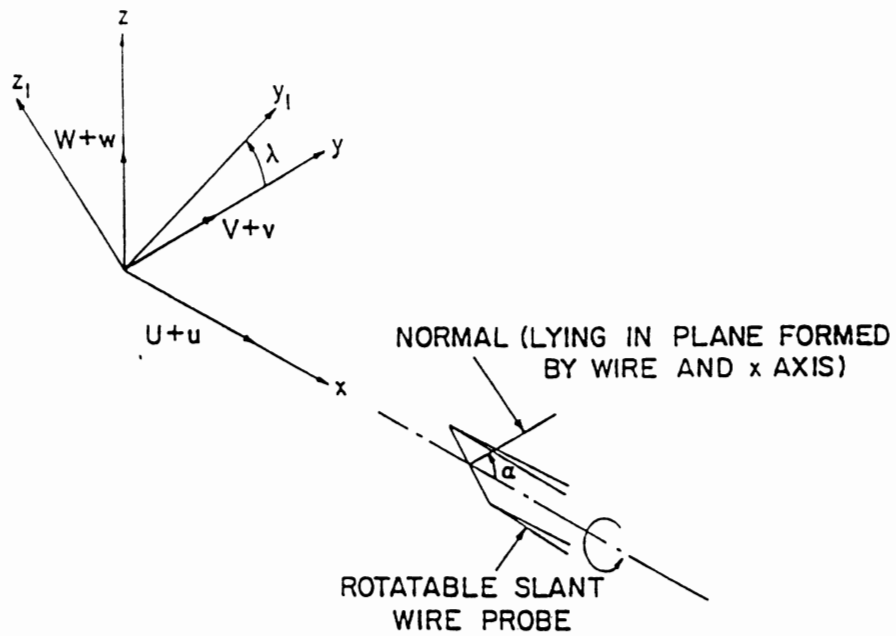

FIG. 1. Reference coordinates *xyz* for probe rotation.

Substituting the expressions of Eq. 2 into a squared version of Eq. 1, and time-averaging the result, yields an expression that relates the wire response to the flow velocity components.

$$\bar{E}^2 = S^2 K_o \bar{U}^2 \left(1 + \frac{\bar{u}^2}{\bar{U}^2} + K_1 \left(\frac{\bar{V}^2}{\bar{U}^2} + \frac{\bar{v}^2}{\bar{U}^2} \right) + 2 K_2 \left(\frac{\bar{V}}{\bar{U}} + \frac{\overline{u v}}{\bar{U}^2} \right) + K_3 h^2 \left(\frac{\bar{W}^2}{\bar{U}^2} + \frac{\bar{w}^2}{\bar{U}^2} \right) \right) \quad (3)$$

where K_o, K_1, K_2 and K_3 are different functions of α and k defined as

$$K_o = \cos^2 \alpha + k^2 \sin^2 \alpha \quad , \quad K_1 = (\sin^2 \alpha + k^2 \cos^2 \alpha) / K_o$$

$$K_2 = (1 - k^2) \sin \alpha \cos \alpha / K_o \quad , \quad K_3 = 1/K_o$$

When the expression of Eq. 3 is utilized with the slant wire measured voltages at each of the four orthogonal positions shown in Fig. 2 (where positions 1 and 2 lie in the x-y plane, while positions 3 and 4 lie in the x-z plane), and combining the expressions for positions 1 and 2, and for positions 3 and 4, the following two coupled non-linear algebraic equations for the mean velocity ratios $\bar{V}/\bar{U}$ and $\bar{W}/\bar{U}$ are obtained

$$K_{0v} + K_{1v} (\bar{V}/\bar{U}) + K_{2v} (\bar{V}/\bar{U})^2 + K_{3v} h^2 (\bar{W}/\bar{U})^2 + C_v = 0 \quad (4)$$

$$K_{0w} + K_{1w} (\bar{W}/\bar{U}) + K_{2w} (\bar{W}/\bar{U})^2 + K_{3w} h^2 (\bar{V}/\bar{U})^2 + C_w = 0 \quad (5)$$

where C_v and C_w are turbulence correction terms given as

$$C_v = K_{0v} (\bar{u}^2/\bar{U}^2) + K_{1v} (\overline{u v}/\bar{U}^2) + K_{2v} (\bar{v}^2/\bar{U}^2) + K_{3v} h^2 (\bar{w}^2/\bar{U}^2) \quad (6)$$

$$C_w = K_{0w} (\bar{u}^2/\bar{U}^2) + K_{1w} (\overline{u w}/\bar{U}^2) + K_{2w} (\bar{w}^2/\bar{U}^2) + K_{3w} h^2 (\bar{v}^2/\bar{U}^2) \quad (7)$$

and $K_{0v}, \cdots, K_{3w}$ are different functions of wire inclination angle α, yaw sensitivity factor k, and measured mean and fluctuation voltage components sensed at the four wire positions.

An expression for the axial mean velocity can be developed by rearranging Eq. 3 and solving for $\bar{U}$ explicitly

$$\bar{U} = \left(\frac{E^2}{S^2 K_o} \right)^{1/2} \left(1 + \frac{\bar{u}^2}{\bar{U}^2} + K_1 \left(\frac{\bar{V}^2}{\bar{U}^2} + \frac{\bar{v}^2}{\bar{U}^2} \right) + 2 K_2 \left(\frac{\bar{V}}{\bar{U}} + \frac{\overline{u v}}{\bar{U}^2} \right) + K_3 h^2 \left(\frac{\bar{W}^2}{\bar{U}^2} + \frac{\bar{w}^2}{\bar{U}^2} \right) \right)^{1/2}$$

A value for $\bar{U}$ can be obtained at each of the four wire positions in Fig. 2. These four values are then averaged to give $\bar{U}$.

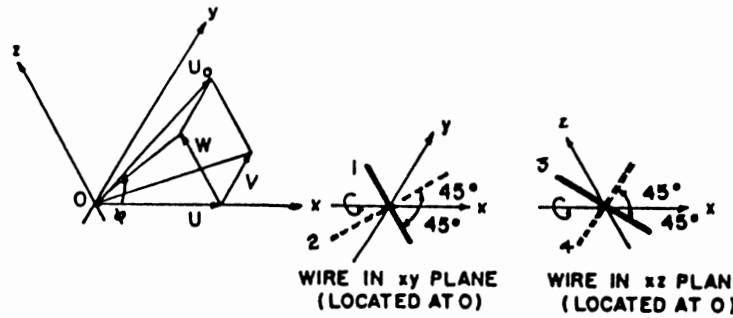

FIG. 2. Slant wire positions for the determination of mean velocity components using single-wire technique.

Different from mean velocity determination, the calculation of the Reynolds stress components is based on rotating the slant wire relative to the plane formed by the x-axis and the resultant transverse mean velocity V_r, defined as shown in Fig. 3. Under these conditions when the effecting cooling velocity expressions is substituted into the following modified form of Eq. 1.

$$\overline{\left(\frac{E^2 - \bar{E}^2}{\bar{E}^2} \right)^2} = \overline{\left(\frac{U\,e^2 - \overline{U\,e^2}}{\overline{U\,e^2}} \right)^2}$$

the following generalized response equation for the six Reynolds stress components referred to the $xy'z'$ coordinates system is obtained,

$$F_{uu}\,(\,\overline{u}^2/\bar{U}^2\,) + F_{vv}\,(\,\overline{v'^2}/\bar{U}^2\,) + F_{ww}\,(\,\overline{w'^2}/\bar{U}^2\,) +$$

$$F_{uv}\,(\,\overline{u\,v'}/\bar{U}^2\,) + F_{uw}\,(\,\overline{u\,w'}/\bar{U}^2\,) + F_{vw}\,(\,\overline{v'w'}/\bar{U}^2\,) = F_{mm} \tag{8}$$

where u, v', w' are the turbulence fluctuation components referred to the coordinate system $xy'\,z'$ and the coefficients F_{uu} through F_{mm} are different functions of α, k, h, θ, $\bar{V}_r/\bar{U}$ and measured mean and fluctuating voltages $\bar{E}$ and $\overline{e}^2$.

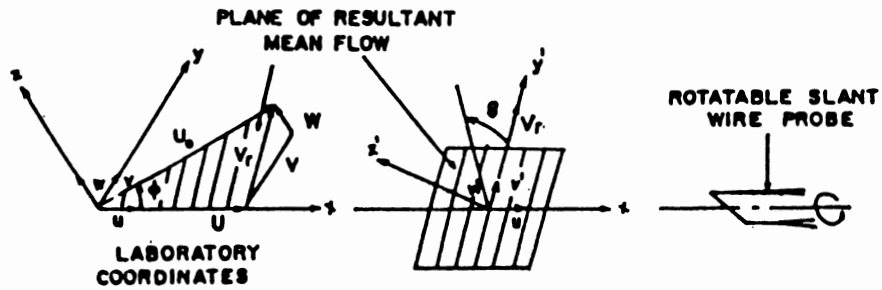

FIG. 3. References coordinates $xy'z'$ for Reynolds stress determination using single wire technique.

In order to solve for the six Reynolds stress components, Eq. 8 must be applied at six different wire positions. These positions are selected in such a way to enhance solution accuracy. Such condition was found to arise when the wire is insensitive (or has weak sensitivity) to a fluctuation component when oriented at certain positions. This system of equations (6×6) in conjunction with Eq. 3-5, constitute nine coupled equations which must be solved for the unknowns $\bar{U}$, $\bar{V}$, $\bar{W}$, $\overline{u}^2$, $\overline{v}^2$, $\overline{w}^2$, $\overline{u\,v}$, $\overline{u\,w}$, $\overline{v\,w}$. The procedure involves transforming Reynolds stresses calculated relative to the $xy'z'$ coordinates to xyz coordinates. The iterative method of solution is described in Ref. [13] in detail.

2.2 X-Wire Technique

This technique is based on the use of a rotatable x-wire probe that consists of two slant wires oriented perpendicular to each other and the planes containing both wires are oriented parallel to each other. It is considered the conventional method of mea-

surement since it is the most common in use among researchers in the experimental field. The technique requires rotation of the probe in certain orientational planes at which measurable voltage components are recorded instantaneously from both wires. When the x-wire probe is aligned parallel to the flow direction and data collected with the plane of both wires A and B lying parallel to the x-y and x-z planes, expressions for the mean velocity and Reynolds stress components are obtained. Subscripts 1 and 2 on E refers to data collected from wires A and B at the x-y plane (positions 1 and 2 in Fig. 2) while subscripts 3 and 4 refers to data collected from wires A and B at the x-z plane (positions 3 and 4 in Fig. 2). Assuming that both wires A and B have similar characteristics[13], the following expressions are obtained,

$$\bar{U}^2 = \frac{\overline{(E_1 + E_2)^2} + \overline{(E_3 + E_4)^2}}{8\ K_o} \tag{9}$$

$$\bar{V}^2 = \frac{\overline{(E_1 - E_2)^2}}{4\ K_o\ K_2^2} \tag{10}$$

$$\bar{W}^2 = \frac{\overline{(E_3 - E_4)^2}}{4\ K_o\ K_2^2} \tag{11}$$

$$\bar{U} = \frac{\bar{E}_1 + \bar{E}_2 + \bar{E}_3 + \bar{E}_4}{4\ \sqrt{K_o}} \tag{12}$$

$$\bar{V} = \frac{\bar{E}_1 - \bar{E}_2}{2\ \sqrt{K_o}\ K_2} \tag{13}$$

$$\bar{W} = \frac{\bar{E}_3 - \bar{E}_4}{2\ \sqrt{K_o}\ K_2} \tag{14}$$

$$\overline{u^2} = \bar{U}^2 - \bar{U}^2 \tag{15}$$

$$\overline{v^2} = \bar{V}^2 - \bar{V}^2 \tag{16}$$

$$\overline{w^2} = \bar{W}^2 - \bar{W}^2 \tag{17}$$

$$\overline{u\,v} = (\bar{E}_1^2 - \bar{E}_2^2) / 4\ K_o - \bar{U}\ \bar{V} \tag{18}$$

$$\overline{u\,w} = (\bar{E}_3^2 - \bar{E}_4^2) / 4\ K_o - \bar{U}\ \bar{W} \tag{19}$$

$$\overline{v\,w} = \frac{\overline{(E_5 - E_6)^2 - (E_7 - E_8)^2}}{8\ K_o\ K_2^2} \tag{20}$$

Detailed derivation of the above equations may be found in Ref. [13].

2.3 Triple-Wire Technique

The technique is based on the development of a real time method which would be applicable to three dimensional flows of unknown flow direction and moderate intensity level. When data obtained from each wire is utilized in Eq. 1, and a proper effective cooling capacity expression in terms of the instantaneous velocity components U, V, and W is substituted, a system of three coupled non-linear algebraic equations is obtained and can be solved for the instantaneous velocities[14].

By using Jorgensen's equation (Eq. 1) for each sensor, one can apply the following equations for each data sample,

$$E_1^2 = S_1^2 \, U_{e1}^2 \tag{21}$$

$$E_2^2 = S_2^2 \, U_{e2}^2 \tag{22}$$

$$E_3^2 = S_3^2 \, U_{e3}^2 \tag{23}$$

where E_1 , E_2 , E_3 are the instantaneous voltage responses sensed by the three wires, and S_1 , S_2 , S_3 are the slopes of the calibration curves for the three wires, respectively.

The triple wire probe has three mutually orthogonal wires arranged to be parallel to the three directions of the wire coordinates system. When the probe holder aligned parallel to the flow direction, the effective velocity sensed by each wire is expressed as

$$U_{e1}^2 = K^2 \, U_{P1}^2 + U_{P2}^2 + h^2 \, U_{P3}^2 \tag{24}$$

$$U_{e2}^2 = h^2 \, U_{P1}^2 + k^2 \, U_{P2}^2 + U_{P3}^2 \tag{25}$$

$$U_{e3}^2 = U_{P1}^2 + h^2 \, U_{P2}^2 + k^2 \, U_{P3}^2 \tag{26}$$

where U_{P1} , U_{P2} , U_{P3} are the instantaneous velocity components parallel to sensors 1, 2, and 3, respectively.

The three non-linear algebraic equations can be solved for the instantaneous velocities U_{P1} , U_{P2} , U_{P3} . Using coordinates transformation, the velocity components referred to wire coordinates are transposed to the velocity components U, V, W referred to the lab-coordinates according to the following

$$U = U_{P1} \cos 45 \cos 35.3 + U_{P2} \cos 45 \cos 35.3 + U_{P3} \sin 35.3 \tag{27}$$

$$V = - U_{P1} \cos 45 + U_{P2} \cos 45 \tag{28}$$

$$W = - U_{P1} \cos 45 \sin 35.3 - U_{P2} \cos 45 \sin 35.3 + U_{P3} \cos 35.3 \tag{29}$$

One the instantaneous values of velocity components are determined, statistical analysis is implemented to calculate the mean velocity components and the six Reynolds stresses according to the following expressions

$$\bar{U} = \frac{1}{N} \sum_{i=1}^{N} U_i \; ; \; \bar{V} = \frac{1}{N} \sum_{i=1}^{N} V_i \; ; \; \bar{W} = \frac{1}{N} \sum_{i=1}^{N} W_i \tag{30}$$

$$\overline{u^2} = \frac{1}{N}\sum_{i=1}^{N} U_i^2 - \bar{U}_i^2 \quad ; \overline{v^2} = \frac{1}{N}\sum_{i=1}^{N} V_i^2 - \bar{V}_i^2 \tag{31}$$

$$\overline{w^2} = \frac{1}{N}\sum_{i=1}^{N} W_i^2 - \bar{W}_i^2 \quad ; \overline{u\,v} = \frac{1}{N}\sum_{i=1}^{N} U_i\,V_i - \bar{U}_i\,\bar{V}_i \tag{32}$$

$$\overline{u\,w} = \frac{1}{N}\sum_{i=1}^{N} U_i\,W_i - \bar{U}_i\,\bar{W}_i \quad ; \overline{v\,w} = \frac{1}{N}\sum_{i=1}^{N} V_i\,W_i - \bar{V}_i\,\bar{W}_i \tag{33}$$

3. Experimental Set-up

A schematic of the test rig is shown in Fig. 4a. A variable speed blower is utilized to control the air flow rate in the chamber. Uniform flow and elimination of any flow irregularities were guaranteed by two fine mesh screens, with one located at the chamber entrance plane while the other is located at an intermediate plane of the 500 mm long, 220 mm diameter chamber, Fig. 4b.

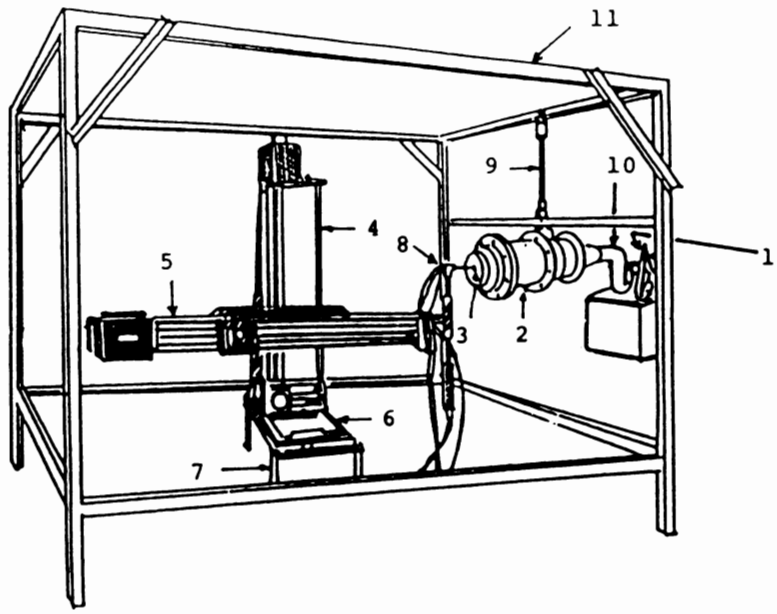

1. Variable speed blower.
2. Settling chamber.
3. Nozzle.
4. Vertical motion traversing mechanism.
5. Axial motion traversing mechanism.
6. Horizontal motion traversing mechanism.
7. Table carrying traverse mechanism.
8. Probe holder.
9. Rod to hold the settling chamber.
10. Flexible hose.
11. Main frame.

FIG. 4(a). Schematic of the test rig.

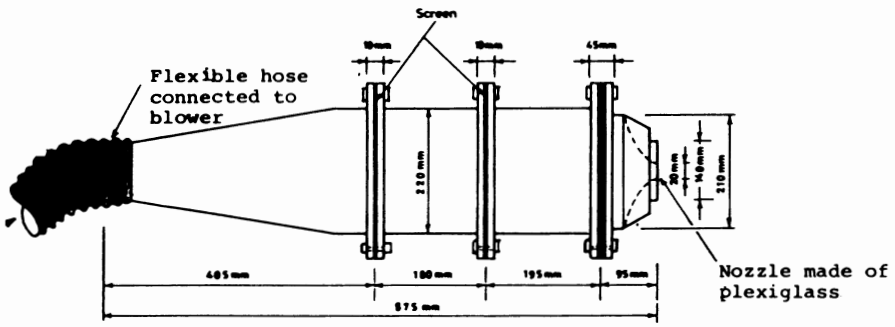

FIG. 4(b). Schematic of the settling chamber and nozzle.

Prior to the data collection phase, single, x, the triple sensor probes were calibrated at the nozzle exit of the jet facility where the velocity profile is essentially uniform with low intensity level. In the calibration process, the jet exit plane velocity was determined by the total head (static head) in the settling plenum by means of a Barocel electronic manometer, in conjunction of a Barocel pressure sensor.

Twelve to twenty values of jet exit velocities were selected such that the velocity range anticipated in the experiment is covered. The calibration points of mean velocity versus measured anemometer voltage is curve fitted with a least squares polynomial of fourth or fifth degrees. The maximum errors obtained by the calibration polynomial was always less than 1% along most of the velocity range except at very low velocities where the uncertainty of calibration results is in the neighborhood of 5%. (This high uncertainty in the lower range of velocities is mainly due to the characteristic non-linear nature of the calibration polynomial).

The traversing system is 57H00 DISA (DANTEC) type mechanism. It has three degrees of freedom enabling three linear motions in three perpendicular directions. Rotational motion was enabled by adopting the DISA type 56H08 unit into the 57H00 traversing mechanism. The unit has a built-in motor driver which was operated automatically by a 386-IBM compatible PC. Accuracy of displacement was measured with a fraction of a mm.

Data acquistion was done using the "acqWIRE" software package developed by DANTEC for turbulent flow measurements. The "acqWIRE" performs data acquisition, traverse control, and calibration, for single-wire, x-wire, triple-wire measurements[14]. The package contains a calibration module that provides the necessary user interface for inputting calibration data for single, x, and triple wire probes. The calibration function is integrated with data processing operations carried out in the experiment to output measured air velocities in laboratory coordinates. The collected data were stored in binary files and then converted later to ASCII files using a software program developed by the authors. Separate programs were developed in order to calculate the mean velocities and the turbulence fluctuation components for the three techniques.

4. Results and Discussion

The main objective of this study is to compare different conventional hot-wire techniques in the measurements of the mean velocity and Reynolds stress components in a flow of moderate intensity level. In order to verify the accuracy of each technique, measurements were conducted near and downstream the exit plane of a free jet exiting from an orifice at axial positions $x/D = 0, 2.5, 5, 10, 15, 20$.

Before measurements were made, preliminary measurements in the near field of the jet were conducted using a normal hot-wire to confirm jet symmetry and to provide mean velocity and turbulence intensity distributions for comparisons with similar results already available in literature. Once jet symmetry was confirmed, measurements were conducted using the three conventional hot-wire techniques. In the data reduction scheme, the pitch sensitivity factor h was specified as constant ($=1$). Since the present study considers a two-dimensional flow with low skewness level ($V/U << 1$), the yaw sensitivity factor was specified as constant ($k = 0.2$) on the basis of extensive calibration data obtained by Al-Beirutty[12].

Figure 5 shows the mean velocity distribution across the jet versus the dimensionless distance r/x at different axial positions from the exit plane ranging from 0 to 25 diameters downstream as measured by a normal hot-wire with its probe aligned parallel to the mean flow. Variation of the local turbulence intensity with the radial position is shown in Fig. 5. The figures show that the mean flow reaches self preservation at $x/D = 10$, while the turbulent fluctuations reach self preservation at further downstream location.

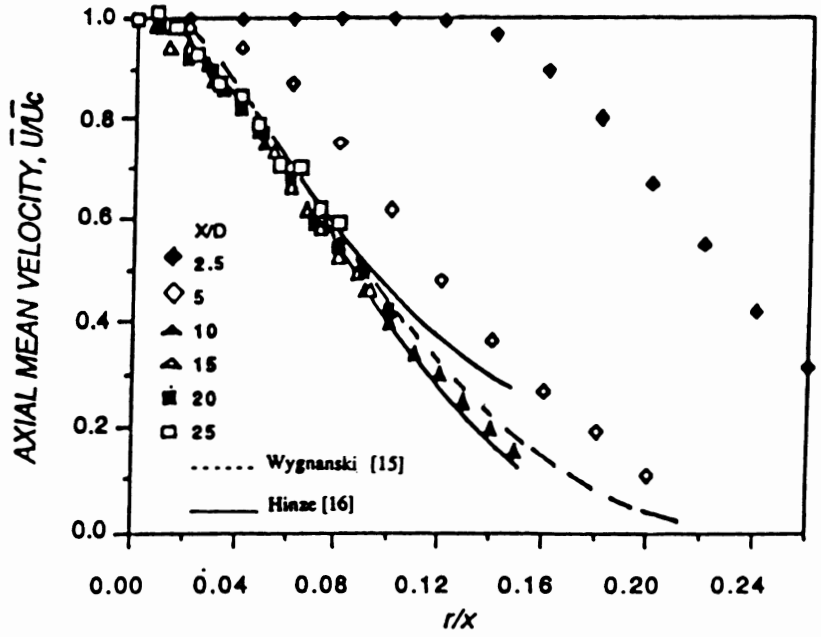

FIG. 5. Comparison of results with published data for $\bar{U}/\bar{U}_c$.

For the sake of comparison, the results of the mean velocity obtained by Wygnanski[15], and Hinze[16] in the preservation region were plotted on Fig. 5. The agreement between the current results and that of Wygnanski and Hinze is quite apparent in the self preservation region ($x/D = 10-25$). In fact, some researchers in the field considered that self preservation starts at $x/D = 20$, but the present study shows that self preservation starts at $x/D = 10$. Similarly, the results for the turbulence intensity $u'/\bar{U}_c$ obtained by Wygnanski[15] and Corrsin[17] are plotted on Fig. 6 for comparison. The coherence of the results for $x/D = 10 - 25$ and the good agreement with the above-mentioned published data even at lower x/D ratio for the self preservation region is a strong proof of the validity of the present results and the accuracy of the measuring instruments.

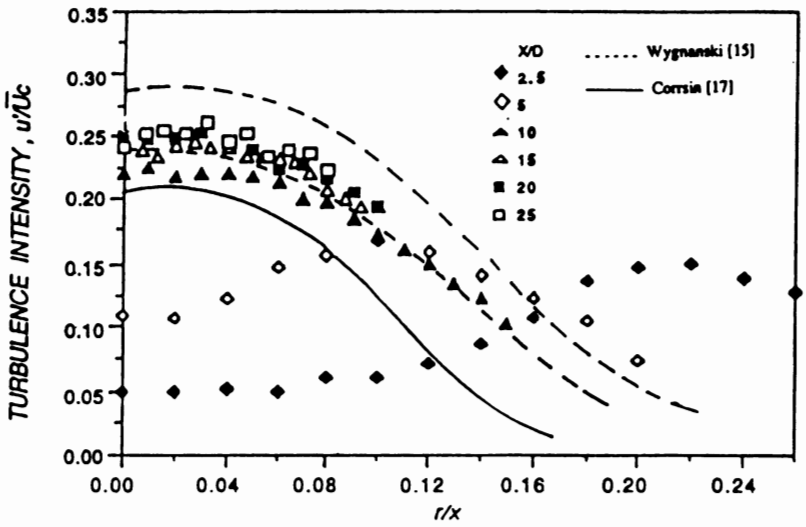

FIG. 6. Comparison of results with published data for $u'/\bar{U}_c$.

Comparison of mean velocity and Reynolds stress components obtained using the three different wire techniques are shown in Fig. 7-11. These figures indicate the symmetry of the flow relative to the measurements coordinate system. The results of the axial mean velocity $\bar{U}$ at different axial locations are shown in Fig. 7. The good agreement among the results indicates that the different wire techniques provide similar accuracy for mean flow measurements when the wire probe is aligned with the mean flow direction, except at $x/D = 5$ where triple wire results significantly deviates from those obtained with single and x-wire techniques. This deviation is also observed for the other results shown in Fig. 7-11, which is attributed to experimental errors at that axial location. The results for the transverse $\bar{V}$ and peripheral $\bar{W}$ mean velocity components were close to zero as measured by the three techniques, therefore, these results are not presented graphically.

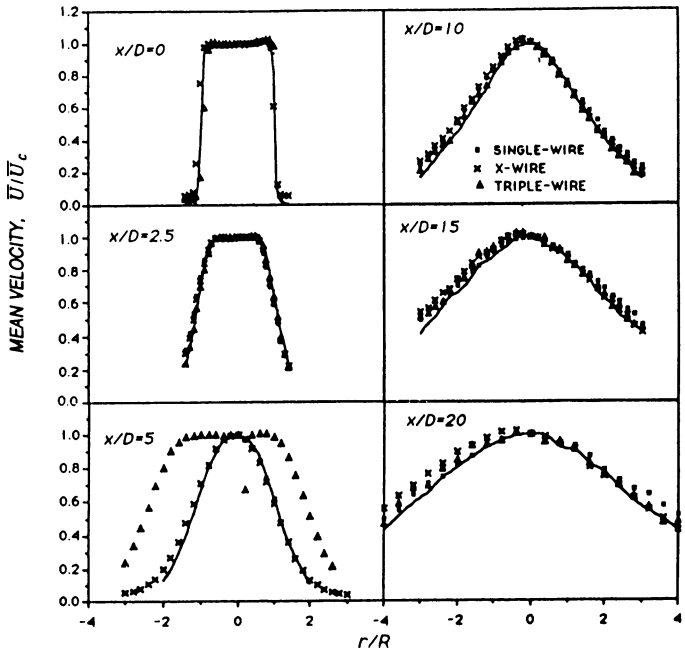

FIG. 7. Mean velocity ($\bar{U}/\bar{U}_c$) distribution across the jet at different axial locations using different hot-wire techniques.

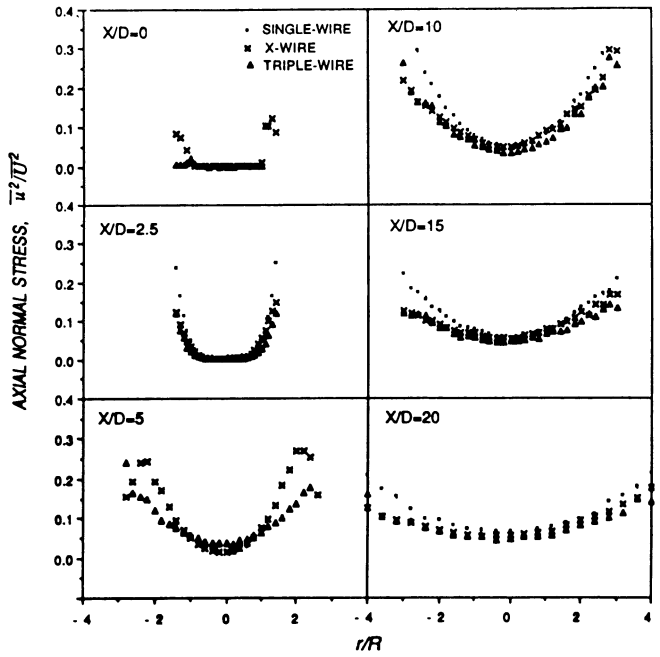

FIG. 8. Axial normal stress ($\overline{u^2}/\bar{U}^2$) distribution across the jet at different axial locations using different hot-wire techniques.

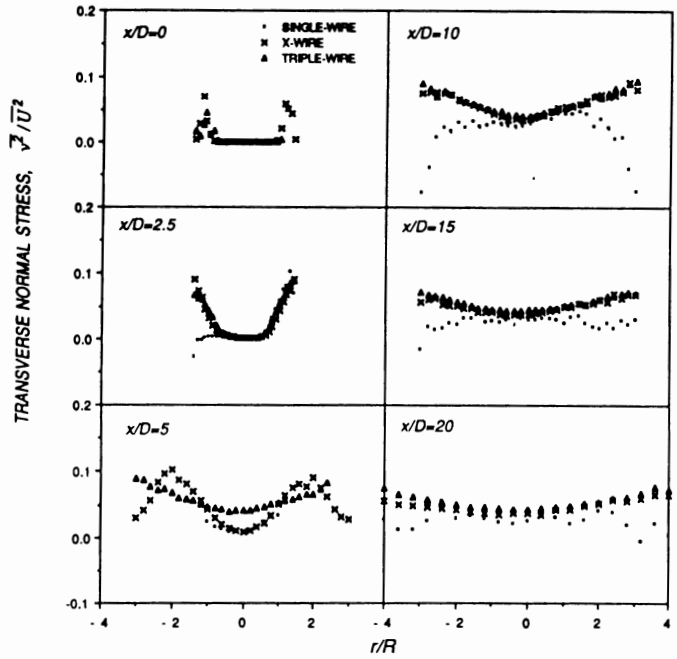

FIG. 9. Transverse normal stress ($\overline{v^2}/\overline{U^2}$) distribution across the jet at different axial locations using different hot-wire techniques.

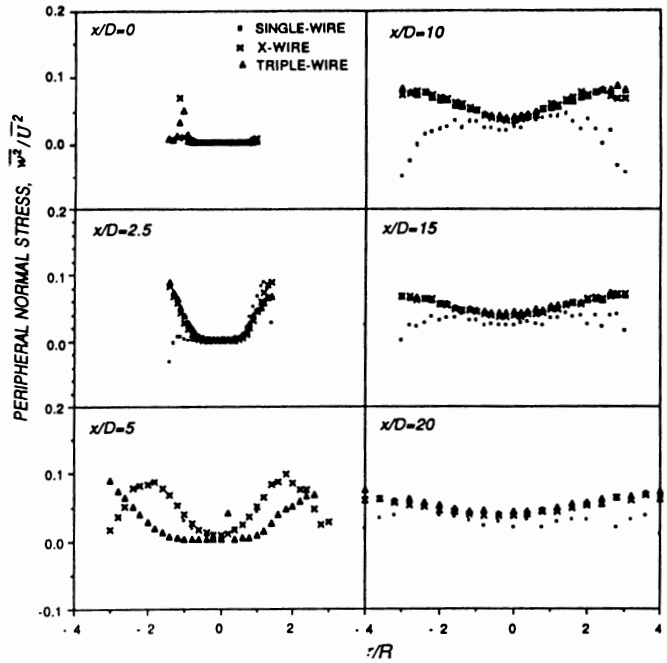

FIG. 10. Peripheral normal stress ($\overline{w^2}/\overline{U^2}$) distribution across the jet at different axial locations using different hot-wire techniques.

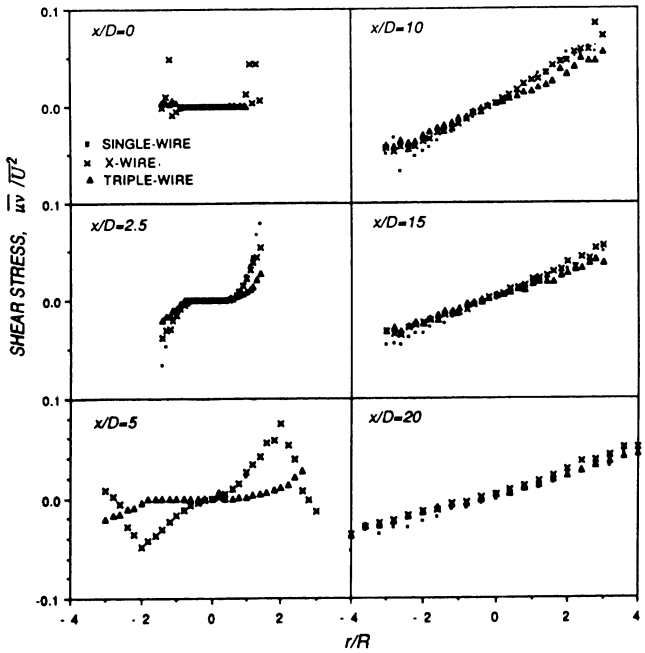

FIG. 11. Shear stress ($\overline{u\,v}/\bar{U}^2$) distribution across the jet at different axial locations using different hot-wire technniques.

Comparison of Reynolds stress components $\overline{u}^2/\bar{U}^2$, $\overline{v}^2/\bar{U}^2$, $\overline{w}^2/\bar{U}^2$, $\overline{u\,v}/\bar{U}^2$, are shown in Fig. 8, 9, 10 and 11, respectively. The agreement among the different techniques is better in a region of larger mean velocity and lower intensity level. However, in a moderate intensity region, the single-wire technique gives higher values of $\overline{u}^2/\bar{U}^2$ than the other techniques. The results obtained by the x-wire and triple-wire techniques are in good agreement for all Reynolds stress components. The large scatter of the transverse, peripheral, and normal stresses especially at large radial positions is due to the large disturbance of the flow caused by the traverse motion during measurements. The pause time length before a data sample was collected after every traverse of the probe was set to 3 seconds when measurements were conducted with a slant-wire. However, it was observed later that the probe holding arm of the traverse vibrates after every traverse and that might have caused some disturbance to the flow and the pause time length was not long enough to eliminate the effect of the probe vibration on the measurements. This problem was eliminated by increasing the pause time length to 10 seconds when measurements were conducted using the x-wire and triple-wire techniques.

In order to perform uncertainty analysis of the results, uncertainties of the calibration variables k, h, α in addition to uncertainties in the measured voltages and calibration polynomial coefficients must be determined first.

In a previous study[12], uncertainty analysis has shown that the mean velocity, normal stress, and shear stress results are the least sensitive to changes (uncertainties) in

the calibration variables while the transverse and binormal stresses are the most sensitive to changes in the calibration variables, and that uncertainties in the yaw sensitivity factor, k ($\pm$ 0.5) has the major contribution to the calculated uncertainties in mean and turbulence quantities.

In this study, it is thought that comparison of the present results to those available in literature would be sufficient to prove the accuracy of the measuring techniques and that uncertainty analysis is not done for this study due to time limitation.

5. Concluding Remarks

The three different hot wire techniques showed good agreement among the results especially for the x-wire and triple-wire techniques. The deviation of the single-wire results for transverse normal stresses were mainly due to experimental and time setting errors as mentioned previously. A good agreement with published results of different investigators was obtained in the self preservation region starting at 10 diameters downstream of the jet exit plane.

Acknowledgement

The authors would like to thank King Abdulaziz University for funding this research work, Project No. 144/409. The patience, understanding and support of the Department of Scientific Research is highly appreciated.

References

[1] **Comte-Bellot, G., Charnay, G.** and **Sabot, J.,** Hot wire and hot film anemometry and conditional measurements, *JFM,* **110,** 115-128 (1981).

[2] **Kawall, J.G., Shokr, M.** and **Keffer, J.F.,** A digital technique for the simultaneous measurement of streamwise and lateral velocities in turbulent flows, *JFM,* **133:** 83-112 (1983).

[3] **Crabb, D., Durao, D.F.G.** and **Whitelaw, J.H.,** A round jet normal to a cross flow, *J. Fluids Engrg. Trans. ASME,* **103**(1): 142-153 (1981).

[4] **Al-Beirutty, M.H., Arterberry, S.H.** and **Gessner, F.B.,** A hot-wire technique for complex turbulent flows, *Proc. First National Fluid Dynamics Congress,* Part 3, AIAA Publications, pp. 1479-1486 (1988).

[5] **Al-Beirutty, M.H.** and **Gessner, F.B.,** A hot-wire measurement technique for moderate intensity, skewed turbulent flows, *Seventh Symp. on Turb. Shear Flows,* Part 2, Stanford University, CA, pp. 19.3.1-19.3.6 (1989).

[6] **Siuru, W.D.** and **Logan, E.,** Use of a slanting hot-wire to make measurements in an artificially roughened tube, *DISA Info.,* **21** (April): 5-10 (1977).

[7] **DeGrande, G.** and **Kool, P.,** An improved experimental method to determine the complete Reynolds stress tenser with a single rotating, slanting hot wire, *J. Phys, E. Sci. Instrum.* **14:** 196-201 (1981).

[8] **Mojola, O.O.,** A hot-wire method for three-dimensional shear flows. *DISA Info.,* **16:** 11-14 (1974).

[9] **Boguslawski, L.** and **Popiel, Cz. O.,** Flow structure in the free-round turbulent jet in the initial region, *JFM,* **90**(part 3): 531-539 (1979).

[10] **Yavuzkurt, S., Crawford, M.E.** and **Moffat, R.J.,** Real time hot wire measurements in three dimensional flows, *Proc. 5th Bienn, Symp. Turb., Univ. of Missouri, Rolla, 1977,* pp. 11.4.1-11.4.10.

[11] **Moffat, R.J., Yavuzkurt, S.** and **Crawford, M.E.,** Real time measurements of turbulence quantities with a triple wire system, *Proc. Dyn. Flow Conf., Johns Hopkins Univ.,* pp. 1013-1035 (Published in Denmark) (1978).

[12] **Al-Beirutty, M.H.,** *Development of a Hot Wire Measurement Technique for Moderate Intensity Three Dimensional Flows,* Ph.D. Thesis, Dept. of Mechanical Eng., Univ. of Washington (1987).
[13] **Al-Beirutty, M., Radwan, A.** and **Khalifa, A.,** *Comparative Studies of Hot-Wire Techniques for Three Dimensional Moderate Intensity Flows,* College of Engineering, KAU, Project No. 144/409 (1990).
[14] **Dantec Elektroniks,** *acqWIRE-Technical Reference Manual,* Allendale, NJ (1989).
[15] **Wygnanski, I.** and **Fiedler, H.,** Some Measurements in the Self-Preserving Jet, *J. Fluid Mech,* **38**(Part 3): 577-612 (1969).
[16] **Hinze, J.O.** and **Van Der Hegge Zijhen, B.G.,** Transfer of heat and matter in the turbulent mixing zone of an axially symmetrical jet, *J. Appl. Sci. Res.*, **A-1:** 435-461 (1949).
[17] **Corrsin, S.** and **Uberoi, M.S.,** *Spectra and Diffusion in a Round Turbulent Jet,* NACA Rept. 1040 (1951).

Nomenclature

D	diameter of nozzle.
E	instantaneous voltage response.
e	voltage fluctuation component.
h	pitch sensitivity factor.
k	yaw sensitivity factor.
r	radial position.
R	radius of nozzle.
S	slope of calibration characteristic.
U, V, W	instantaneous velocity components in x, y, z directions, respectively.
u, v, w	fluctuating velocity components in x, y, z directions, respectively.
U_{BN}	binormal velocity component, wire coordinates.
U_e	effective cooling velocity.
U_N	normal velocity component, wire coordinates.
U_p	parallel velocity component, wire coordinates.
u^2, v^2, w^2	Reynolds normal stress quantities referred to xyz coordinates
uv, uw, vw	Reynolds shear stress quantities referred to xyz coordinates.
V_r	resultant transverse velocity.
x, X	axial position.
$x\ y\ z$	laboratory coordinate system.
$x\ y'\ z'$	optimum coordinate system.
α	angle between probe axis and normal to wire.
ϕ	flow angle ($\phi = \tan^{-1}(V_r/U)$).
λ	wire rotation angle (relative to lab. coordinates $x\ y\ z$).
θ	wire orientation angle (relative to opt. coordinates $x\ y'\ z'$)
$\overline{(\quad)}$	time-averaged quantity.
$(\quad)$	fluctuation quantity referred to x, y', z' coordinates, or RMS value.

دراسة مقارنة لتقنية السلك الحراري الساخن في تدفق ذي شدة اضطراب متوسطة

محمد حسين البيروتي ، و عبد الحي محمد رضوان
و عادل محمد خليفة

قسم الهندسة الميكانيكية ، كلية الهندسة ، جامعة الملك عبدالعزيز
جدة – المملكة العربية السعودية

المستخلص . توجد طرق متعددة لاستخدام تقنية السلك الساخن للحصول على معلومات عن التدفق المضطرب للموائع . واختبرت هذه التقنيات في حالات وأشكال متعددة وتحت ظروف تشغيليه مختلفة . وقد وُجد أنه من الصعب تفضيل تقنية معينة على أخرى مالم يتم اختبار التقنيات المختلفة تحت نفس الحالات والظروف .

إن الهدف الرئيس لهذه الدراسة يتلخص في مقارنة القياسات والنتائج باستخدام تقنية الأسلاك الساخنة المنفردة بنظيرتها ، الناتجة عن استخدام الأسلاك المزدوجة والثلاثية تحت نفس الحالات والظروف التشغيلية .

وقد تم قياس مركبات متوسط السرعة في الاتجاهات الثلاثة ، وإجهاد رينولدز عند سبعة نقاط على الخط المحوري من مخرج منفث هوائي ، باستخدام السلك المنفرد والسلك المزدوج والسلك الثلاثي ، وقد تم التحكم في جهاز تحريك السلك الساخن باستخدام الكمبيوتر ، إضافة إلى تطوير برنامج لتجميع معلومات قياسات السريان المضطرب وتحليلها .

وقد أظهرت نتائج التقنيات الثلاثة نتائج متشابهة ومتقاربة بالنسبة لقيم مركبات متوسط السرعة ومركبات إجهاد رينولدز في الأبعاد الثلاثة ، إلا أنه لوحظ أن هذا التقارب والتوافق في النتائج لم يكن ظاهرًا في مركبات الإجهاد العمودية ، وبالذات في حالة تقنية السلك المنفرد . وقد تم الحصول على توافق جيد عند مقارنة نتائج متوسط المركبة المحورية (UU_c) وشدة الاضطراب (u'/U_c) مع النتائج المنشورة لباحثين آخرين . وهذا التوافق أكد الثقة والدقة في طرق القياسات التي استخدمت في هذه الدراسة .